

# A Comparative Study of Classical and Advanced MPPT Control Algorithms for Photovoltaic Systems

**Abstract.** This paper is aimed to study and compare the performance of four different Maximum Power Point Tracking (MPPT) techniques used to extract the maximum power from photovoltaic (PV) systems. The MPPT methods considered in this study include Perturb and Observe (PO), Fuzzy Logic Control (FLC), Sliding Mode Control (SMC) and Fuzzy Sliding Mode Control (FSMC). A PV model and DC-DC power converter are modelled in Matlab Simpower Systems toolbox and the MPPT algorithms are tested under different operating conditions to analyse the performance and limitations of each algorithm.

**Streszczenie.** W artykule przedstawiono porównanie właściwości czterech technik MPPT – Maximum Power Point Tracking stosowanych do sterowania systemami fotowoltaicznymi. Te cztery techniki były symulowane i analizowane w różnych warunkach pracy. **Analiza porównawcza metod MPPT stosowanych w systemach fotowoltaicznych**

**Keywords:** Photovoltaic, MPPT, Fuzzy Logic, Sliding mode, Boost converter.

**Słowa kluczowe:** systemy fotowoltaiczne, techniki MPPT – Maximum Power Point Tracking

## Introduction

Traditionnally, electrical energy is produced mainly from fossil fuels and nuclear power plants. Due to the increasing demand of energy worldwide, there has been an excessive consumption of these resources during the last century which has led to considerable pollution of the atmosphere with a significant impact on the environment [1], [2]. Since these primary source of energy are non-renewable and rapidly declining, it is necessary to explore other solutions to satisfy the continuously increasing demand of energy. The aim is therefore to have an economic, sustainable and less-polluting source of energy, since the protection of the environment has also become a serious concern [3].

The search for new energy resources is one of the priorities of the energy policy of many countries. Renewable energies represent a viable alternative to fossil fuels and could provide electricity everywhere [4].

Solar energy, which is available in abundance over the entire surface of the earth, despite a significant decrease in the crossing of the atmosphere; the quantity that arrives on the ground remains quite important. Solar irradiance can reach 1000 W/m<sup>2</sup> peak in temperate zones and up to 1400 W/m<sup>2</sup> when the atmosphere is slightly polluted. Currently, photovoltaic (PV) technology is become mature and more advanced. The basic elements are cells or photovoltaic panels that convert solar radiation into electric current [5]. Maximum Power Point Tracking (MPPT) controllers allow PV system to work at maximum power points of their characteristics without prior knowledge of these operating points and their variation following changing weather conditions [6]. MPPT is a principle for tracking the maximum power point of a nonlinear electrical generator in order to force the generator to work at its maximum power (MPP). Indeed, this operation makes it possible to obtain the best power output of the cell.

There are several MPPT algorithms in the literature based on methods such as: Hill-Climbing, Perturb & Observ, (P&O) [7] - [9], fuzzy logic (FLC) [10] - [15], sliding mode (SMC) [16] ], [17] and fuzzy logic sliding mode (FSMC) [6], [18], [19], super twisting Sliding mode control (STSMC), integral Sliding mode control (ISMC), double integral Sliding mode control (DISMC), higher order SMC [6], [19] - [22].

According to the literature search it was found that the classic P&O method is the most widely used because of its

simplicity and ease of implementation [5] but its major disadvantage is that it is not robust against parameter variations such as the meteorological data (temperature and irradiances). To overcome this problem several advanced techniques have been proposed to improve the performance of MPPT and also ensure its robustness. Among these, FLC-based MPPT is often used [15], due to its robustness and also it does not require any prior information about the studied system.

In addition, MPPTs based on non-linear control theory have also been proposed recently [19]. They tend to be more robust and give better performance under variable in the weather conditions. The only drawback of this MPPT is that they tend to produce excessive fluctuations due to the chattering phenomenon [20]. To overcome this problem several combinations have been proposed including: Fuzzy logic control (FLC), Sliding Mode Control (SMC), Fuzzy Sliding Mode Control (FSMC), Super Twisting Sliding Mode Control (STSMC), Integral Sliding Mode Control (ISMC), Double Integral Sliding Mode Control (DISMC) and higher order Sliding Mode Control (HOSMC).

In this paper, a combination of the classical P&O type control with advanced algorithms such as FLC, SMC and FSMC is proposed to determine the best configuration in terms of both performance and robustness against variations of meteorological data.

The paper is structured as follows: Section 1 on the description and modeling of the photovoltaic conversion system. Section 2 presents the mathematical modeling of the PV system and its MPPT control. Section 3 presents the different MPPT algorithms. In Section 4, the simulation results are presented and an interpretation is made to evaluate the contributions of the MPPT methods studied in the paper. Finally, the conclusion of the paper is presented in Section 5 .

## 2. Photovoltaic Conversion System

The photovoltaic conversion system consists of four building blocks as shown in Fig. 1. The first block represents the energy source (photovoltaic panel), the second block is a DC / DC adaptation stage, the third block represents the load and the fourth block represents the control system. The matching stage operates in such a way that the panel delivers the maximum energy.

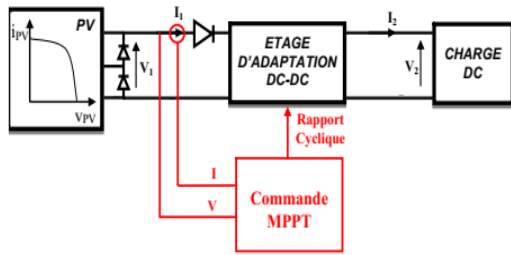


Fig. 1 : Basic structure of the PV conversion system.

### 2.1. Modeling of the PV Array

The electric power generated from the PV array fluctuates with the operating conditions and field factors such as the sun's position angle, irradiation levels and ambient temperature. A solar cell can be represented as a current source model as shown in Fig. 2.

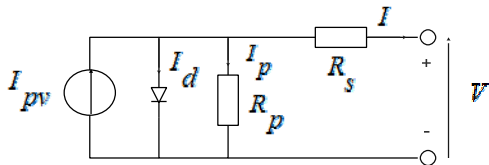


Fig. 2 Single-diode equivalent circuit of a PV cell.

Applying Kirchhoff's current law, the terminal current of the cell is [4], [23]:

$$(1) \quad I = I_{pv} - I_d - I_p$$

$$(2) \quad I_p = \frac{V + R_s I}{R_p}$$

The junction current is given by:

$$(3) \quad I_d = I_0 \left[ e^{\left( \frac{V + R_s I}{V_t \alpha} \right)} - 1 \right]$$

The formula relating the current and voltage in the circuit is:

$$(4) \quad I = I_{pv} - I_0 \left[ e^{\left( \frac{V + R_s I}{V_t \alpha} \right)} - 1 \right] - \frac{V + R_s I}{R_p}$$

$$(5) \quad V_t = \frac{N_s K T}{q}$$

The light generated current of the PV cell depends linearly on the solar irradiation and is also dependent on the temperature according to the following equation [4], [6], [7]:

$$(6) \quad I_{pv} = (I_{pv,n} + K_I \Delta T) + \frac{G}{G_n}$$

The diode saturation current and its dependence on the temperature may be expressed by:

$$(7) \quad I_0 = \frac{I_{sc,n} + K_I \Delta T}{\left( \frac{I_{oc,n} + K_V \Delta T}{\alpha V_t} \right) - 1}$$

The parameters and model constants of the KC200GT solar array, used in this study, are given in the Appendix.

### 2.2. Maximum Power Point Tracking

Fig. 3 shows the basic circuit configuration of a DC-DC boost converter with an MPPT controller. A capacitor is generally connected between PV panel and the boost circuit to reduce high frequency harmonics.

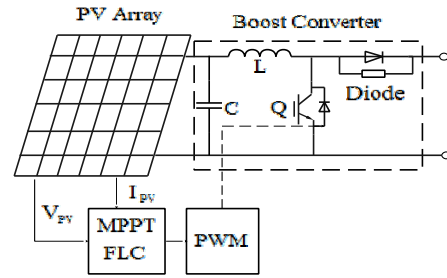


Fig. 3 Boost converter circuit and MPPT control.

## 3. MPPT Command Algorithms

### A. MPPT based on P&O

The principle of this algorithm is to perform a disturbance on the voltage of the

PV panel while acting on the duty cycle  $\alpha$ . Indeed, following this disturbance, the power supplied by the PV panel is calculated at time  $k$ , and then compare to the previous one of the moment  $(k - 1)$ .

If the power increases, we approach the point of maximum power, 'PMP' and the variation of the duty cycle is maintained in the same direction.

On the contrary, if the power decreases, we move away from the point of maximum power, 'PMP'. Then, we must reverse the direction of the variation of the duty cycle [7]. Table 1 summarizes the operation of the P&O algorithm.

Table 1. the operation of the P&O algorithm

Case	$dP_{pv}$	$dV_{pv}$	Action	duty cycle
1	$P(k) > P(k-1)$	$V(k) > V(k-1)$	V++	D--
2	$P(k) > P(k-1)$	$V(k) < V(k-1)$	V--	D++
3	$P(k) < P(k-1)$	$V(k) > V(k-1)$	V--	D++
4	$P(k) < P(k-1)$	$V(k) < V(k-1)$	V++	D--

### B. MPPT based on FLC

Similar FLC-based MPPT controllers have been proposed in [10] - [15]. The basic structure of a FLC is shown in Fig. 4. The inputs are the error  $E$  and error change  $dE$ ; the output is the PWM duty cycle variation  $dD$ .

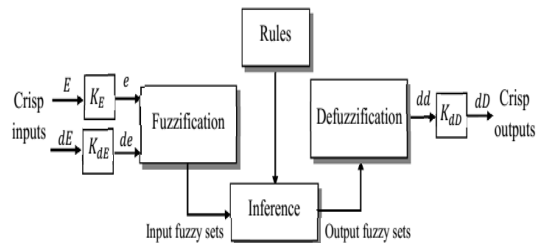


Fig. 4 Building blocks and structure of a FLC.

In Fig. 4  $K_E$ ,  $K_{dE}$  and  $K_{dD}$  are scaling gains selected to achieve the desired transient and steady-state response characteristics [6], [12]- [14], [16]. The universe of discourse for each input and output variable is divided into five fuzzy sets defined by triangular membership functions and labelled as NB (Negative Big), NS (Negative Small), ZE (Zero), PS (Positive Small) et PB (Positive Big) as shown in Fig. 5. The fuzzy rules used to determine the controller output are summarized in Table 2. The defuzzification is based on the popular centre of gravity method.

Table. 1 Fuzzy control rules.

E \ dE	dE				
	NB	NS	ZE	PS	PB
NB	ZE	ZE	PB	PB	PB
NS	ZE	ZE	PS	PS	PS
ZE	PS	ZE	ZE	ZE	NS
PS	NS	NS	NS	ZE	ZE
PB	NB	NB	NB	ZE	ZE

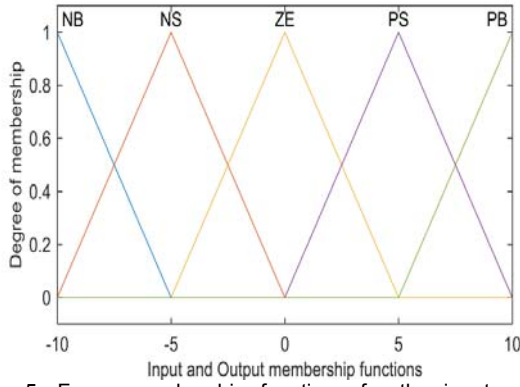


Fig. 5. Fuzzy membership functions for the input and output variables.

### C. MPPT based on SMC

SMC is an effective nonlinear robust control approach which provides system dynamics with an invariance property to uncertainties once the system dynamics are controlled in the sliding mode.

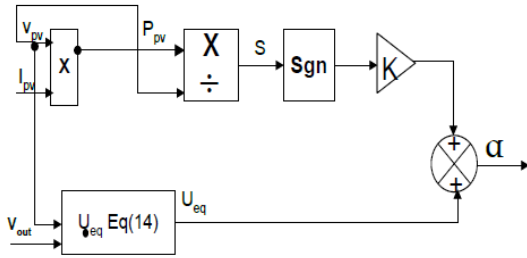


Fig. 6 Building blocks and structure of a SMC.

The first step of SMC design is to select a sliding surface that models the desired closed-loop performance in state variable space. Then the control should be designed such that the system state trajectories are forced towards the sliding surface and stay on it. The system state trajectory during the period of time before reaching the sliding surface is called the reaching phase. Once the system trajectory reaches the sliding surface, it stays on it and slides along it to the origin. The system trajectory sliding along the sliding surface to the origin is the sliding mode. The structure of a sliding mode controller is defined by [10]:

$$(8) \quad U = U_{eq} + U_n$$

where:  $U_{eq}$  is called equivalent control.  $U_n$  is called normal control.

The structure of a sliding mode controller is defined by [17]:

$$(9) \quad U = \alpha(k+1) \quad \text{and} \quad U_{eq} = \alpha(k)$$

with  $\alpha(k+1)$  and  $\alpha(k)$  is the duty cycle in the instants  $k$  and  $k+1$  respectively.

The switching function ( $S$ ) defined as:

$$(10) \quad S = \frac{[\partial P]_{pv}}{[\partial V]_{pv}}$$

With

$$(11) \quad P_{pv} = V_{pv} * I_{pv}$$

Substituting equation (11) in equation (10) gives:

$$(12) \quad S = \frac{\partial(V_{pv} * I_{pv})}{\partial V_{pv}} = V_{pv} \left( \frac{[\partial I]_{pv}}{[\partial V]_{pv}} + I_{pv} / V_{pv} \right)$$

The switching function in the instant  $k$  and  $k+1$  respectively becomes:

$$(13) \quad S = V_{pv} \left( \frac{(I_{pv}(k) - I_{pv}(k-1))}{(V_{pv}(k) - V_{pv}(k-1))} + \frac{I_{pv}(k)}{V_{pv}(k)} \right)$$

The duty cycle of boost is :

$$(14) \quad \alpha = 1 - (V_{in}) / (V_{out})$$

The equivalent control of the MPPT\_SMC is the expression for the duty cycle is obtained as follows:

$$(15) \quad U_{eq} = \alpha$$

The normal control ( $U_n$ ) it is defined as:

$$(16) \quad U_n = K * \text{sgn}(S)$$

$K$  is a positive constant, representing the maximum controller output required to overcome parameter uncertainties and disturbances. The basic SMC scheme is shown in Fig. 6.

### D. MPPT based on FSMC

This MPPT control strategy is a combination of FLC and SMC. In order to eliminate the chattering phenomenon inherent in the SMC, the  $\text{sgn}$  block of the SMC (Fig. 6) is replaced by the FLC block as illustrated in Fig. 7.

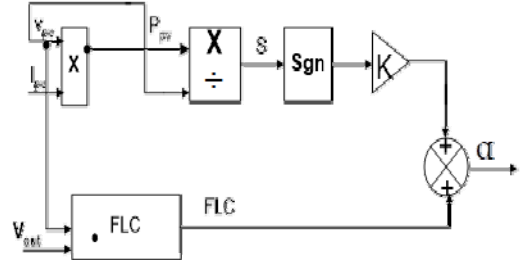


Fig. 7 Building blocks and structure of a FSMC

## 4. Simulation Results and Discussion

The PV conversion system and MPPT control schemes studied are simulated in Matlab/Simulink and SimpowerSystem toolbox with the parameters given in the Appendix. This simulation study will be based on three scenarios: (i) constant weather conditions ( $T = 25^\circ\text{C}$  and  $R = 1000 \text{ W/m}^2$ ), (ii)  $T$  variable and  $R$  constant and (iii)  $T$  constant and variable  $R$ .

Under these conditions, the performance of the MPPT controllers will be assessed according to their performances, speed (response time to the transient regime), robustness to parameter variations and the presence of oscillations around the optimal values of the electrical quantities studied (Powers, voltages and currents of the photovoltaic panel and boost converter).

### (i) Scenario 1: Constant weather conditions

The results are shown in Fig. 8.

- Between  $t = 0 \text{ s}$  and  $t = 0.02 \text{ s}$  the voltage  $V_{pv}$  is unstable for all MPPT methods and in particular for SMC where the voltage peak exceeds 30 V.

- When  $t > 0.02 \text{ s}$ , the voltage  $V_{pv}$  begins to stabilize around its average value which exceeds 26 V for all MPPT methods but with less chattering with FLC, SMC and FSMC as compared P&O as shown in Fig. 10.

- at  $t = 0 \text{ s}$ , it can be notice that the current  $I_{pv}$  for exceeds 8 A for all MPPTs and almost reaches the value of  $I_{sc,R} = 8.21 \text{ A}$ . Between  $t = 0$  and  $0.02 \text{ s}$ , the SMC exhibits a significant negative peak amplitude of about 4 A whereas the currents for the other MPPT controllers have amplitudes varying between 1.5 A and 2 A.

- When  $t > 0.02 \text{ s}$  the current  $I_{pv}$  starts to stabilize for all commands but with less chattering in the case of FLC, SMC and FSMC as compared to the P&O method as shown in Fig. 10.

It can be noted that the power of the boost converter with P&O method does not reach its optimum average value (185.32 W) that after a time ( $t = 50 \text{ ms}$ ) with ripples of amplitude of  $\pm 0.87 \text{ W}$ .

The power of the boost converter with FLC boost reaches its optimum average value of 189.02 W after a time  $t = 40 \text{ ms}$ . Note that this time is less than that of P&O with amplitude ripples of the order of  $\pm 0.4 \text{ W}$ . On the other hand, for SMC and FSMC the powers have the same average optimal value 189.04 W.

These results are illustrated by Fig.11.

Between  $t = 0 \text{ s}$  and  $t = 0.04 \text{ s}$ , the SMC and FSMC based MPPTs have a shorter response time of  $V_{boost}$  equal to 10 ms as compared to FLC and P&O where the response times are 40 ms and 50 ms respectively.

For  $t > 0.4 \text{ s}$ , the voltage  $V_{boost}$  begins to stabilize around its average value for all MPPT controllers as shown in Fig. 12. From  $t = 0.1 \text{ s}$  the current  $I_{boost}$  starts to stabilize at its average value for all the MPPT control schemes but it is lower than the current  $I_{pv}$ .

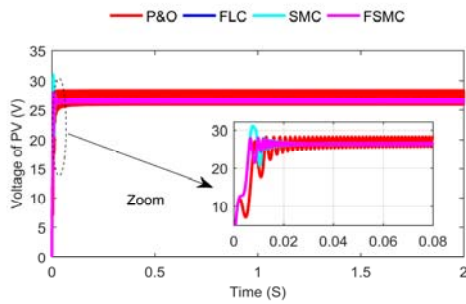


Fig. 8 Voltage of PV with T ET R constants.

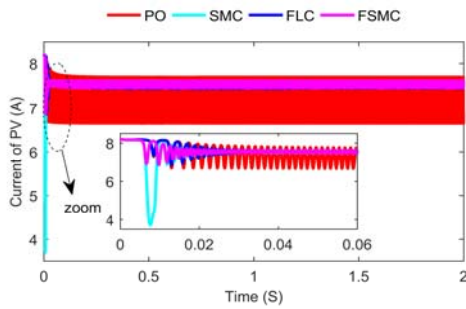


Fig. 9 Current of PV with T ET R constants.

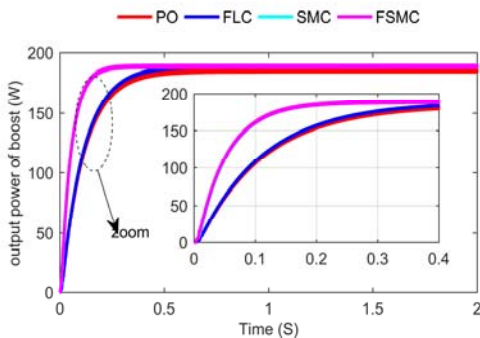


Fig. 10 Output power of Boost with T et R constants.

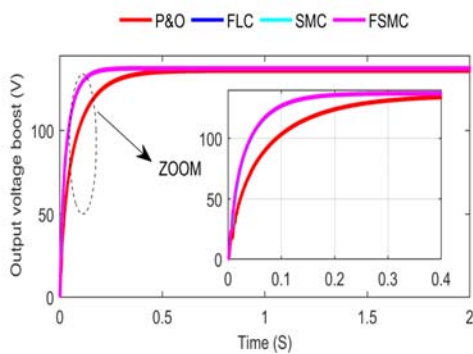


Fig. 11 Output voltage of Boost with T et R constants.

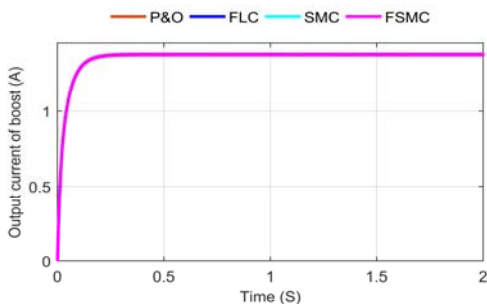


Fig. 12 Output current of Boost with T et R constants.

(ii) **Scenario 2-  $T = 25$  and  $40^{\circ}\text{C}$  and  $R = 1000 \text{ W/m}^2$**

The results are shown in Fig. 13. In this scenario,  $R = 1000 \text{ W/m}^2$  and the temperature is varied from  $25^{\circ}\text{C}$  to  $40^{\circ}\text{C}$ . After a time ( $t = 0.1\text{s}$ ), the powers of the FSMC and SMC controls begin to stabilize around their new optimal average value compared to the other two MPPT methods (FLC and P&O) and they will appear more robust to these variations. A slight decrease in their power amplitudes of all controls. The FLC based MPPT remains the best method to minimize the chattering amplitudes.

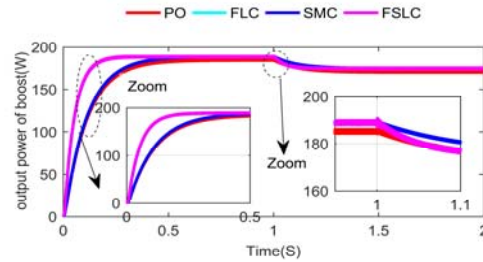


Fig. 13 Power of Boost with T variable.

(iii) **Scenario 3 -  $T = 25$  and  $R = 1000 \text{ W / m}^2$  and  $600 \text{ W / m}^2$**

The results are presented in Fig. 14.

In this scenario,  $T$  is set at  $25^{\circ}\text{C}$  and  $R$  is varied from  $1000 \text{ W/m}^2$  to  $600 \text{ W / m}^2$ . After a time  $t = 0.15 \text{ s}$ , the powers of the FSMC and SMC controls begin to stabilize around their new optimum average value compared to the other two (FLC and P&O) and they will appear more robust to these variations. A significant decrease in the power amplitudes of all controls can be observed. The FLC-based MPPT controller remains the best approach to minimize the chattering amplitudes.

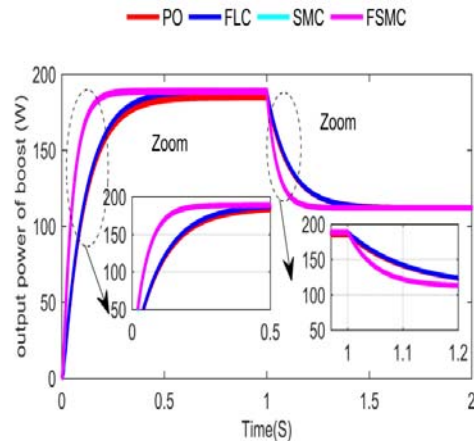


Fig. 14 Power of Boost with R variable.

**5. Conclusions**

In this paper a four MPPT algorithms (PO, SMC, FLC, FSLC) has been evaluated for tracking MPPs of a PV system. The simulation results show that improved performance has been achieved by these algorithms as compared to P&O. P&O method can cause large ondulation caused by discontinuous control law and a of the parametrs system are actually known. SMC, FLC, FSLC methods provides better performance and robustness even under large temperature and irradiation changes. For any algorithms, more simulation results will be presented and discussed by considering other operating conditions with a comparative study between the proposed MPPT strategies.

**Acknowledgment**

The authors would like to acknowledge the financial support of the Algeria's Ministry of Higher Education and Scientific Research. This work was supported by SCAMRE laboratory at Polytechnic national school (Oran, Algeria) in collaboration with L2GEGI laboratory at the University Ibn-Khaldun (Tiaret, Algeria).

## Appendix

Parameters of the model of the PV

Type	KC200GT	
$P_{max}[W]$	200.143	
$(V_{oc,n}) [V]$	32.9	
$(I_{sc,n}) [A]$	8.21	
$I_{c,n}[A]$	$9.825 \cdot 10^{-8}$	
$R_p[\Omega]$		415.405
$R_s[\Omega]$		0.221
$K_v[V/K]$	-0.123	
$K_i[A/K]$	0.0032	
$\alpha$	1.3	
$N_s$	54	
DC/DC converter parameters		
Chopper type		Boost
Semiconductor switch type		IGBT
Converter inductor		11 $\mu$ H
Converter capacitor		1mF

## Nomenclature

$P_{pv}$	Photovoltaic system output power
$V_{pv}$	Photovoltaic system output voltage
$I_{pv}$	Photovoltaic current
$I_d$	Diode current
$I_c$	Saturation current
$I_{c,n}$	Nominal saturation current
$I_{sc,n}$	Nominal short-circuit current
$V_{oc,n}$	Nominal open circuit voltage
$R_s$	Series resistance
$R_p$	Parallel resistance
$K_v$	Voltage coefficient
$K_i$	Current coefficient
$V_t$	Thermal voltage
$A$	Diode ideality factor
$N_s$	Cells connected in series
$K$	Polarization voltage
$T$	Temperature
$Q$	Electron charge
$C$	Input filter capacitance of PV converter
$L$	Inductive filter
$V_{oc}$	DC-link voltage
$I_{oc}$	DC-link current
$P_{load}$	Load power
$P$	Real power

## Authors

**Abderrahmane HEBIB**, Department of Electrical Engineering, Faculty of Electrical Engineering, He is Ph.D. in Electrical Engineering. His research interests are renewable energy and applications of intelligence technique in Photovoltaic Systems; He is a member in SCAMRE Laboratory at ENP, Oran, Algeria. Email: [oueldallal@hotmail.com](mailto:oueldallal@hotmail.com)

**Allaoui Tayeb**, Professor of Electrical Engineering, Electrical Engineering Department, He is a Director of Energetic Engineering and Computer Engineering Laboratory at the Ibn Khaldoun University of Tiaret, Algeria. Email: [allaoui\\_tb@yahoo.fr](mailto:allaoui_tb@yahoo.fr)

**Abdelkader CHAKER**, Professor of Electrical Engineering, Electrical Engineering Department, He is a Director of SCAMRE Laboratory at ENP, Oran, Algeria. Email: [chakeraa@yahoo.fr](mailto:chakeraa@yahoo.fr)

**Belkacem BELABBAS**, is a lecturer in the Department of Electrical Engineering. His research activities include the Renewable Energies and the Control of Electrical Systems. He is a member in Energetic Engineering and Computer Engineering Laboratory at the Ibn Khaldoun University of Tiaret, Algeria. Email: [belabbas.belkacem@yahoo.fr](mailto:belabbas.belkacem@yahoo.fr)

**Denai Mouloud**, is a Senior Lecturer in Electric Power and Control. He graduated from the University of Science and Technology of Algiers and Ecole Nationale polytechnique of Algiers, Algeria in Electrical Engineering, and received his PhD in Control Engineering from the University of Sheffield, UK, He is currently with the School of Engineering & Technology, University of Hertfordshire, UK. Email: [m.denai@herts.ac.uk](mailto:m.denai@herts.ac.uk)

## REFERENCES

- [1] H. Wu, S. Wang, B. Zhao, et C. Zhu, « Energy management and control strategy of a grid-connected PV/battery system », *Int. Trans. Electr. Energy Syst.*, 2014.
- [2] M. Coppola et al., « Maximum Power Point Tracking Algorithm for Grid-tied Photovoltaic Cascaded H-bridge Inverter », *Electr. Power Compon. Syst.*, vol. 43, n° 8, p. 951–963, 2015.

- [3] T. Kerekes, D. Séra, et L. Máthé, « Three-phase Photovoltaic Systems: Structures, Topologies, and Control », *Electr. Power Compon. Syst.*, vol. 43, n° 12, p. 1364–1375, 2015.
- [4] N. Eghtedarpour et E. Farjah, « Control strategy for distributed integration of photovoltaic and energy storage systems in DC micro-grids », *Renew. Energy*, vol. 45, p. 96–110, 2012.
- [5] N. Karami, N. Moubayed, et R. Outbib, « General review and classification of different MPPT Techniques », *Renew. Sustain. Energy Rev.*, vol. 68, p. 1–18, 2017.
- [6] M. Arsalan, R. Iftikhar, I. Ahmad, A. Hasan, K. Sabahat, et A. Javeria, « MPPT for photovoltaic system using nonlinear backstepping controller with integral action », *Sol. Energy*, vol. 170, p. 192–200, 2018.
- [7] H. E. A. Ibrahim et M. Ibrahim, « Comparison Between Fuzzy and P&O Control for MPPT for Photovoltaic System Using Boost Converter », *J. Energy Technol. Policy*, vol. 2, n° 6, p. 1–11, 2012.
- [8] H.-T. Yau, Q.-C. Liang, et C.-T. Hsieh, « Maximum power point tracking and optimal Li-ion battery charging control for photovoltaic charging system », *Comput. Math. Appl.*, vol. 64, n° 5, p. 822–832, 2012.
- [9] A. G. Abo-Khalil, D.-C. Lee, J.-W. Choi, et H.-G. Kim, « Maximum power point tracking controller connecting PV system to grid », *J. Power Electron.*, vol. 6, n° 3, p. 226–234, 2006.
- [10] B. Belabbas, T. Allaoui, M. Tadjine, et M. Denai, « Power management and control strategies for off-grid hybrid power systems with renewable energies and storage », *Energy Syst.*, p. 1–30, 2017.
- [11] B. Belabbas, T. Allaoui, M. Tadjine, et M. Denai, « Power Quality Enhancement in Hybrid Photovoltaic-Battery System based on three-Level Inverter associated with DC bus Voltage Control », *J. Power Technol.*, vol. 97, n° 4, p. 272–282, 2017.
- [12] F. A. O. Aashoor et F. V. P. Robinson, « Maximum power point tracking of photovoltaic water pumping system using fuzzy logic controller », in *Power Engineering Conference (UPEC), 2013 48th International Universities*, 2013, p. 1–5.
- [13] M. Ouada, M. Meridjet, M. Saoud, et N. Talbi, « Increase efficiency of photovoltaic pumping system based BLDC motor using fuzzy logic MPPT control », *WSEAS Trans Power Syst.*, vol. 8, p. 104–113, 2013.
- [14] M. Ouada, M. S. Meridjet, et N. Talbi, « Optimization photovoltaic pumping system based BLDC using fuzzy logic MPPT control », in *Renewable and Sustainable Energy Conference (IRSEC), 2013 International*, 2013, p. 27–31.
- [15] H. Al-Raweshidy et M. Abbod, « A Novel Maximum Power Point Tracking Technique based on Fuzzy logic for Photovoltaic Systems », 2018.
- [16] M. Farhat, O. Barambones, et L. Sbita, « A new maximum power point method based on a sliding mode approach for solar energy harvesting », *Appl. Energy*, vol. 185, p. 1185–1198, 2017.
- [17] T. ESRAM, P. L. Chapman, et others, « Comparison of photovoltaic array maximum power point tracking techniques », *IEEE Trans. ENERGY Convers. EC*, vol. 22, n° 2, p. 439, 2007.
- [18] M. Mohammadi et M. Nafar, « Fuzzy sliding-mode based control (FSMC) approach of hybrid micro-grid in power distribution systems », *Int. J. Electr. Power Energy Syst.*, vol. 51, p. 232–242, 2013.
- [19] A. Kchaou, A. Naamane, Y. Koubaa, et N. M'sirdi, « Second order sliding mode-based MPPT control for photovoltaic applications », *Sol. Energy*, vol. 155, p. 758–769, 2017.
- [20] B. Yang et al., « Perturbation observer based fractional-order sliding-mode controller for MPPT of grid-connected PV inverters: Design and real-time implementation », *Control Eng. Pract.*, vol. 79, p. 105–125, 2018.
- [21] H. Zhang et S. Cheng, « A new MPPT algorithm based on ANN in solar PV systems », in *Advances in Computer, Communication, Control and Automation*, Springer, 2012, p. 77–84.
- [22] A. B. G. Bahgat, N. H. Helwa, G. E. Ahmad, et E. T. El Shenawy, « Maximum power point tracking controller for PV systems using neural networks », *Renew. Energy*, vol. 30, n° 8, p. 1257–1268, 2005.
- [23] Q. Mei, M. Shan, L. Liu, et J. M. Guerrero, « A Novel Improved Variable Step-Size Incremental-Resistance MPPT Method for PV Systems », *Ind. Electron. IEEE Trans. On*, vol. 58, n° 6, p. 2427–2434, 2011.